

Title	Negative magnetoresistance of Be -doped GaAs structures
Author(s)	Idutsu, Y; Noh, J.P; Shimogishi, F; Otsuka, N
Citation	Physical Review B : Condensed Matter and Materials Physics, 73(11): 115306-1-115306-6
Issue Date	2006-03
Type	Journal Article
Text version	publisher
URL	http://hdl.handle.net/10119/3352
Rights	Y. Idutsu, J. P. Noh, F. Shimogishi, and N. Otsuka, Physical Review B, 73(11), 115306, 2006. Copyright 2006 by the American Physical Society. http://scitation.aip.org/getabs/servlet/GetabsServlet?prog=normal&id=PRBMD000007300011115306000001&idtype=cvips&gifs=Yes
Description	



Negative magnetoresistance of Be δ -doped GaAs structures

Y. Idutsu, J. P. Noh, F. Shimogishi, and N. Otsuka*

School of Materials Science, Japan Advanced Institute of Science and Technology, Asahidai 1-1, Nomishi, Ishikawa 923-1292, Japan

(Received 12 September 2005; revised manuscript received 30 November 2005; published 3 March 2006)

Magnetotransport properties of Be δ -doped structures grown by molecular-beam epitaxy have been studied in the temperature range from 5 K to room temperature. In the structure, an ultrathin low-temperature-grown GaAs layer or Se δ -doped layer are placed in the vicinity of a Be δ -doped layer, which results in a strong localization of holes at deep levels of the Be δ -doped layer. With an applied magnetic field perpendicular to the δ -doped layer, positive magnetoresistance is observed at all measured temperatures. With an applied magnetic field parallel to the δ -doped layer, on the other hand, negative magnetoresistance occurs from room temperature to nearly 100 K, below which magnetoresistance changes into positive values. The negative magnetoresistance with a parallel magnetic field results from localized spins in the Be δ -doped layer. Bumps of curves of magnetoresistance are observed with parallel magnetic fields in the temperature range from 50 to 100 K, which suggests the possibility of antiferromagnetic alignments of the spins in δ -doped layer.

DOI: 10.1103/PhysRevB.73.115306

PACS number(s): 71.30.+h

I. INTRODUCTION

In recent years active researches have been carried out in the field of diluted magnetic semiconductors (DMS's) based on III-V compounds, aimed at the incorporation of the spin degree of freedom in semiconductor electronics.^{1–3} In DMS's transition metal elements which possess localized spins are placed as substitutional atoms in tetrahedrally coordinated semiconductor crystals. Solubilities of these magnetic elements as substitutional atoms in the III-V semiconductor crystals are generally low. A great deal of effort, therefore, has been made for an increase in their concentration in DMS's in order to raise the Curie temperature.

It has been known since the early time of researches on impurity-doped semiconductors that even nonmagnetic shallow impurities such as P in Si possess localized spins by forming hydrogenic states at low temperatures. Direct evidence of the existence of localized spins at these shallow impurity states was obtained by electron paramagnetic resonance (EPR) experiments.^{4–6} By electron nuclear double resonance experiments, these spins were found to form antiferromagnetic coupling at higher impurity concentrations.⁷ At a still higher impurity concentration a metal-insulator transition occurs as a result of significant overlapping of impurity wave functions.⁴ The existence of localized spins and their antiferromagnetic coupling occur only at very low temperatures because of thermal excitation of carriers from shallow impurity levels to either a conduction band or valence band.

In recent studies we have found a transition from thermally activated conduction to metallic conduction at room temperature in Be δ -doped structures grown by molecular-beam epitaxy (MBE).^{8–10} Here the metallic conduction simply implies the positive dependence of the resistivity on the temperature, and, hence, this transition is not necessarily a metal-insulator transition in the strict sense. The structure is made of a combination of a Be δ -doped layer and an ultrathin low-temperature-grown GaAs(LT-GaAs) layer or a Se δ -doped layer with a 1-nm-thick spacer layer between them. The transition occurs with a change in the Be doping con-

centration among samples from a lower range to a higher range of 10^{13} cm^{-2} . A LT-GaAs layer is known to contain a high concentration of deep donor antisite arsenic atoms (As_{Ga}), and Se becomes shallow donors in GaAs. A part of holes in the Be δ -doped layer are hence trapped by As_{Ga} atoms or Se atoms, leaving heavy holes only at deep levels of the Be δ -doped layer. The thermally activated conduction at room temperature implies that these holes are strongly localized and that they participate in the conduction via thermal excitation to extended states.

There may be a number of factors leading to strong localization of holes in the Be δ -doped structures. All of these factors may not be easily identified, but one important factor can be attributed to the formation of squeezed hydrogenic states at deep levels of the δ -doped layer. The width of the triangular potential well at deep levels of the δ -doped layer with a high Be concentration in the order of 10^{13} cm^{-2} is nearly 1 nm according to self-consistent calculations of electron states.¹⁰ At a deep level, therefore, a Be ion and a heavy hole form a quasi-two-dimensional hydrogenic state whose Bohr radius is known to be smaller than that of the three-dimensional case.^{11,12} As a result of this, heavy holes are localized in each hydrogenic impurity state even at high Be doping concentrations due to insufficient overlapping of impurity wave functions.

According to the aforementioned earlier EPR studies, therefore, one can expect existence of localized spins in the Be δ -doped structures at high temperatures and also their antiferromagnetic coupling at higher Be concentrations. In the present paper we report results of the magnetotransport study which has been carried out in order to investigate these possibilities. The most direct evidence of the existence of localized spins may be obtained by either EPR experiments or measurements of magnetic susceptibility, but densities of δ -doped Be atoms in these samples each of which we expect to have a localized spin are only in the order of 10^{13} cm^{-2} .⁸ Such densities are too low to be detected by the above-mentioned experiments, in particular, at high temperatures considered here. We have, therefore, employed magne-

totransport measurements with magnetic fields applied in both perpendicular and parallel directions with respect to a δ -doped layer. With an applied magnetic field perpendicular to the δ -doped layer, positive magnetoresistance was observed at all measured temperatures. With an applied magnetic field parallel to the δ -doped layer, on the other hand, negative magnetoresistance was observed from room temperature to nearly 100 K, below which magnetoresistance became positive. The negative magnetoresistance with a parallel magnetic field results from localized spins in the Be δ -doped layer where localized holes are considered to form hydrogenic states at Be atoms. In addition to these results, we observed bumps of curves of magnetoresistance in the temperature range between 50 and 100 K, which suggests a possibility of antiferromagnetic alignments of these localized spins.

II. EXPERIMENT

Figure 1(a) schematically shows a sample structure. Thicknesses of layers are written in parentheses. Samples were grown by utilizing a conventional MBE system. Semiconducting epiready (100) GaAs wafers were used as substrates and mounted on a Mo holder with indium. A Ga flux and As flux for the growth were 5.8×10^{-7} Torr and 3.0×10^{-5} Torr, respectively, which gave rise to a growth rate of $0.9 \mu\text{m}/\text{h}$. After desorption of an oxide layer of the substrate surface, the surface was annealed for 10 min at 600 °C, followed by the growth of a 150-nm-thick GaAs buffer layer at 580 °C. After growth of the buffer layer, the substrate temperature was lowered to a temperature in the range from 300 °C to 520 °C for the δ -doping of Be and Se and growth of a spacer layer and cap layer. In the case of the growth of an ultrathin LT-GaAs layer and LT-GaAs cap layer, the substrate temperature was further lowered to 150 °C. More detailed explanations of the growth experiments were given in earlier papers.^{8,10}

Figure 1(b) shows a representative energy diagram of a Be δ -doped structure which was obtained by a self-consistent calculation based on the Schrödinger equation and Poisson equation. For the calculation, the Be δ -doped concentration and donor δ -doped concentration were assumed as $6.3 \times 10^{13} \text{ cm}^{-2}$ and $3.2 \times 10^{13} \text{ cm}^{-2}$, respectively. The Be δ -doped layer and donor δ -doped layer are located at positions of 0 and +1 nm in the figure, respectively. Detailed procedures of the calculation are explained in an earlier paper.¹⁰ In the figure E_1 and E_2 denote bottoms of the first and second subbands of heavy holes, respectively, and E_F indicates the Fermi energy. Subbands of light holes are located at shallower levels, and the density of states for light holes which is proportional to the effective mass is far smaller than that for heavy holes. In this δ -doped structure, therefore, deep levels are occupied mainly by heavy holes as shown in Fig. 1(b).

A square 5 mm × 5 mm sample was cut for the van der Pauw measurements of resistivity of samples, and an In contact was made at each corner of a sample.⁸ For magnetoresistance measurements, a Physical Property Measurement System (PPMS) was used. A rectangular 3 mm × 8 mm

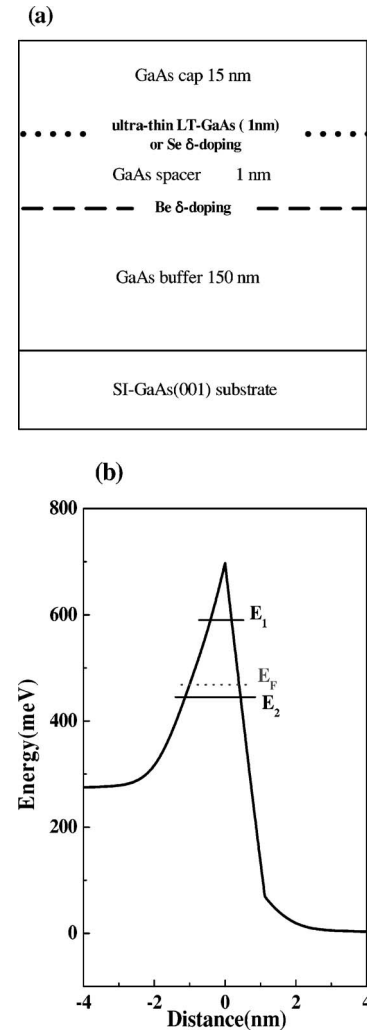


FIG. 1. (a) Layer configuration of a Be δ -doped structure. Thicknesses of layers are written in parentheses. (b) Energy diagram of a Be δ -doped layer and donor δ -doped pair structure which is obtained by the self-consistent calculation. In the figure, the Be δ -doped layer and donor δ -doped layer are located at 0 and +1 nm.

sample was cut, and four In contacts were made with an equal spacing in the longitudinal direction for these measurements. All samples described in the present paper exhibit *p*-type conduction and hence have holes as current carriers.

III. RESULTS AND DISCUSSION

Figure 2 shows the temperature dependence of resistivity of three Be δ -doped structures in each of which an ultrathin LT-GaAs layer is placed near the Be δ -doped layer. These three samples, called Be/LT-1, Be/LT-2, and Be/LT-3, were used for the magnetoresistance measurements. Sheet hole densities of these samples which were estimated by Hall effect measurements are $8.90 \times 10^{12} \text{ cm}^{-2}$, $3.27 \times 10^{12} \text{ cm}^{-2}$, and $1.45 \times 10^{12} \text{ cm}^{-2}$, respectively. Two samples Be/LT-2 and Be/LT-3 exhibit thermally activated conduction in the entire measured temperature range and hence correspond to insulating samples. The sample Be/LT-1, on the other hand, exhibits positive temperature dependence in the high-

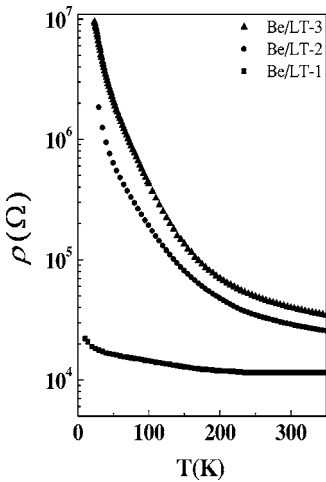


FIG. 2. Temperature dependence of resistivity of the sample Be/LT-1, Be/LT-2, and Be/LT-3.

temperature side. Beryllium doping concentrations of Be/LT-1, Be/LT-2, and Be/LT-3 are $6.50 \times 10^{13} \text{ cm}^{-2}$, $8.64 \times 10^{13} \text{ cm}^{-2}$, and $4.95 \times 10^{13} \text{ cm}^{-2}$, respectively. The Be δ -doping of the sample Be/LT-1 was carried out at 450°C , while those of the other two samples were made at 520°C , which resulted in the metallic conduction of the sample Be/LT-1 in spite of its low Be concentration. Arrhenius plots of the resistivity of the samples Be/LT-2 and Be/LT-3 as well as their Hall mobility show three different temperature ranges with respect to conduction processes as reported in the earlier paper.⁸ In the temperature range from 350 K to approximately 150 K, the Arrhenius plots become linear with activation energies for the conduction being a few tens meV. In this temperature range the conduction occurs via thermal excitation of localized holes to extended states where the mobility is ranged from $50 \text{ cm}^2/\text{s V}$ to $80 \text{ cm}^2/\text{s V}$. In the temperature range below 50 K activation energies and mobility become very low, indicating the dominance of hopping conduction in this low-temperature range. In the temperature range between the above two ranges, namely the range from 50 to 150 K, the conduction process is considered to change from the former to the latter.

Figure 3(a) shows the temperature dependence of the resistivity of two Be δ -doped structures in which a Se δ -doped layer is placed in place of an ultrathin LT-GaAs layer. These samples have higher resistivity than that of the transition at room temperature and hence belong to insulating samples. Sheet hole densities of these two samples Be/Se-1 and Be/Se-2 at room temperature are $6.89 \times 10^{12} \text{ cm}^{-2}$ and $3.56 \times 10^{12} \text{ cm}^{-2}$, respectively. As seen in the figure, these samples exhibit resistivity maxima. As the substrate temperature for the δ -doping and growth of a spacer and a cap layer is raised from 350°C to 500°C , the resistivity maxima have become more pronounced forms. The Hall mobility of the samples also has increased with an increase in the substrate temperature. Among all samples with Be and Se δ -doped layers, the two samples shown in Fig. 3(a) exhibit the most pronounced resistivity maxima. Figure 3(b) shows the temperature dependence of the Hall mobility of the sample Be/Se-2. As seen in the figure the mobility mono-

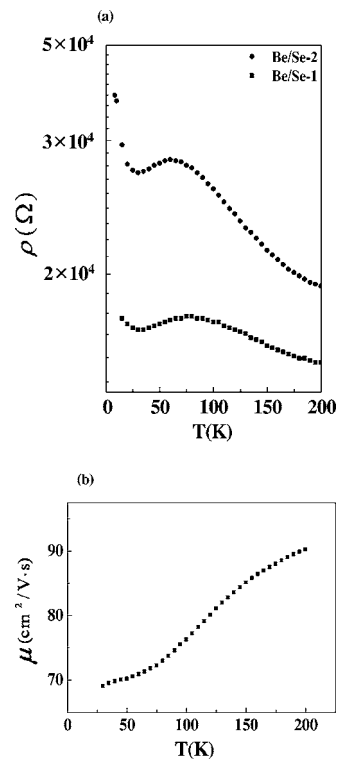


FIG. 3. (a) Temperature dependence of resistivity of two Be δ -doped samples with Se δ -doped layers. (b) Temperature dependence of the Hall mobility of the sample Be/Se-2.

tonically changes with the temperature with the *p*-type conduction in spite of the occurrence of the resistivity maxima. The Be doping concentrations of these two samples are $3.24 \times 10^{13} \text{ cm}^{-2}$, where the Se doping concentration of the former sample is lower than that of the latter sample. The accurate estimation of the Se concentrations in these samples was not made because of the less-than-unity sticking coefficient of Se on a GaAs surface which changed sensitively to the flux condition and substrate temperature.¹⁰

The magnetoresistance of a sample was estimated by measuring resistance of the sample from 300 to 5 K under fixed magnetic fields 4.5 and 9 T and subtracting the resistance measured under the zero magnetic field from the former. Magnetic fields parallel to the δ -doped layer were applied in the direction perpendicular or parallel to the current. At selected temperatures, magnetoresistance was measured as a function of the applied field B . Figure 4(a) shows the temperature dependence of magnetoresistance of the sample Be/LT-2 for perpendicular and parallel magnetic fields B_\perp and B_\parallel of 9 T. As seen in the figure, there is distinct anisotropy of magnetoresistance between perpendicular and parallel fields. Magnetoresistance of the perpendicular field is positive at all measured temperatures and monotonically increases by lowering the temperature. The rapid increase below 100 K is attributed to the large positive magnetoresistance of hopping conduction which results from the distortion of wave functions of localized carriers by an applied magnetic field.¹³ Magnetoresistance of the parallel field, on the other hand, is negative in the temperature range above 100 K where the negative magnetoresistance monotonically

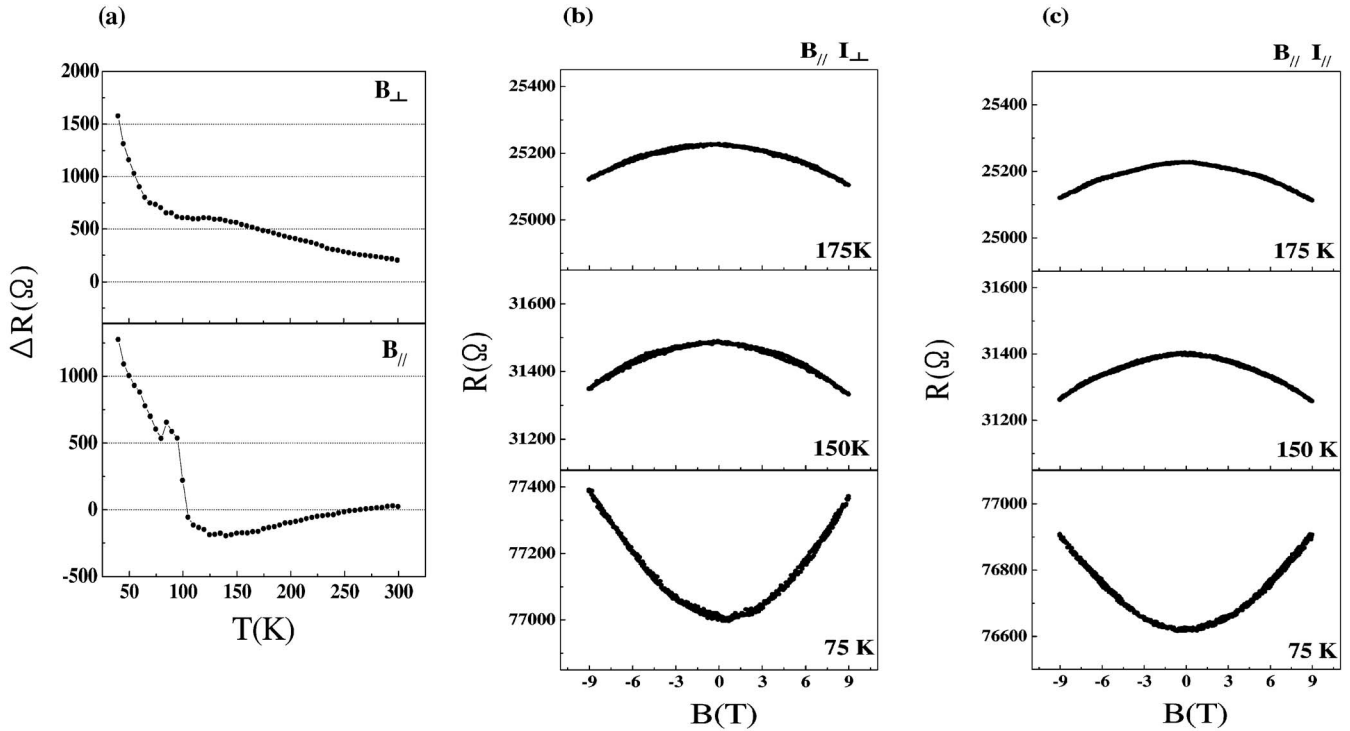


FIG. 4. (a) Temperature dependence of perpendicular and parallel field magnetoresistance of the sample Be/LT-2. Resistance of the sample Be/LT-2 as a function of the parallel field B with the field (b) perpendicular and (c) parallel to the current for 175, 150, and 75 K.

increases by lowering the temperature from 300 to 125 K. Below 100 K the magnetoresistance becomes positive and rapidly increases at lower temperatures which may also be ascribed to the positive magnetoresistance of hopping conduction. In Figs. 4(b) and 4(c), the field dependence of magnetoresistance is plotted under the parallel field condition for 175, 150, and 75 K. Plots in Fig. 4(b) were obtained with the applied field perpendicular to the current, while those in Fig. 4(c) with the applied field parallel to the current. Magnitudes of magnetoresistance in Figs. 4(b) and 4(c) are nearly identical to each other for a given temperature in spite of the difference in the direction of the magnetic field with respect to the current. For the remaining samples, therefore, only results of magnetoresistance with the applied field perpendicular to the current are presented.

Figure 5(a) is the temperature dependence of the parallel field magnetoresistance of the samples Be/LT-1 and Be/LT-3. The strength of the magnetic field is 9 T. Similarly to the sample Be/LT-2, both samples exhibit negative magnetoresistance in the temperature ranges from 300 to 80 K. The magnetoresistance of the sample Be/LT-3 could not be measured at a temperature below 80 K because values of the resistance for both 0 and 9 T exceeded the measurement limit of the PPMS instrument at these temperatures. The tendency of the temperature dependence of the negative magnetoresistance of three samples are similar to one another, but the value of the negative resistance becomes greater as the sample resistance is higher as seen in Figs. 4(a) and 5(b). In Fig. 5(b) negative magnetoresistance of the sample Be/LT-1 was plotted as a function of $1/T^2$. Values of magnetoresistance in this figure were obtained from measurements of resistance as a function of the applied field for given temper-

tures, with which accurate values of magnetoresistance were obtained by minimizing the effect of the temperature variation.

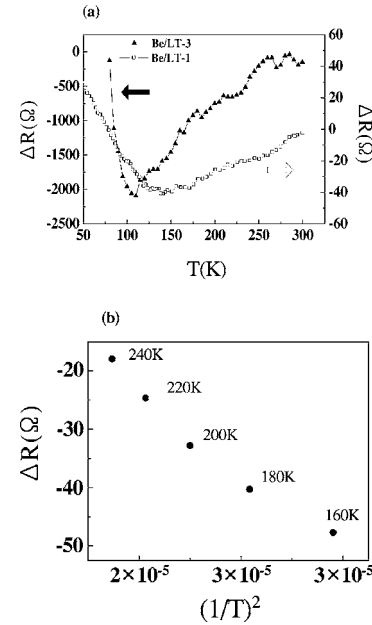


FIG. 5. (a) Temperature dependence of parallel field magnetoresistance of the sample Be/LT-1 and Be/LT-3. The strength of the magnetic field is 9 T. (b) Plots of negative magnetoresistance of the sample Be/LT-1 against $1/T^2$ in the high temperature side. A value of negative magnetoresistance was derived from the measurement of resistance as a function of the field for each temperature.

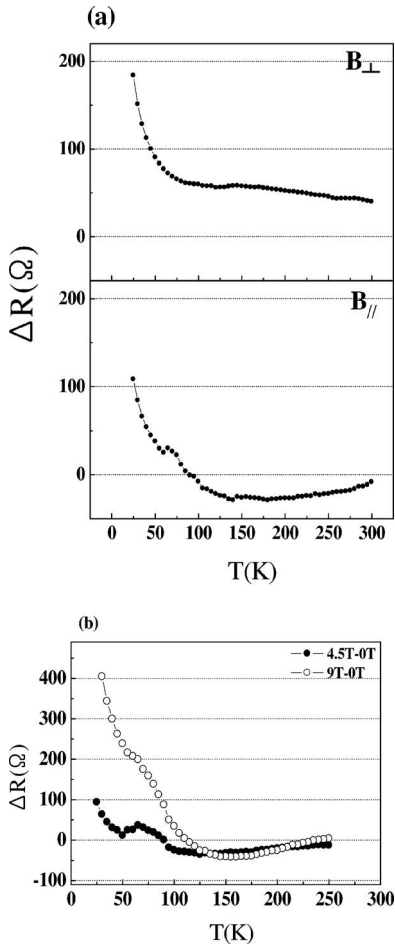


FIG. 6. (a) Temperature dependence of perpendicular and parallel field magnetoresistance of the sample Be/Se-1. The strength of the magnetic field is 9 T. (b) Temperature dependence of the parallel field magnetoresistance of the sample Be/Se-2 for magnetic fields 4.5 and 9 T.

In Fig. 6(a) the temperature dependence of magnetoresistance of the sample Be/Se-1 is shown for both perpendicular and parallel magnetic fields of 9 T. The negative magnetoresistance is again observed at higher temperatures under the parallel magnetic field. At temperatures below 100 K the parallel field magnetoresistance becomes positive and again exhibits a small bump around 70 K. Figure 6(b) shows the temperature dependence of the parallel field magnetoresistance of the sample Be/Se-2 for 4.5 and 9 T. The curve of 4.5 T shows a bump around 70 K, while that of 9 T has a shoulder around this temperature.

The anisotropy between the perpendicular and parallel field magnetoresistance in the high temperature range is observed from all examined samples. In addition, as shown in Fig. 4(b) and 4(c), similar negative magnetoresistance is observed in the two cases where the applied field is perpendicular and parallel to the current, although only in the latter case the coupling of the field with the orbital motion of carriers is completely inhibited. This implies that the negative magnetoresistance occurs in a nearly two-dimensional structure. Similar negative magnetoresistance is observed from both Be/LT samples and Be/Se samples. This indicates that the

negative magnetoresistance occurs in Be δ -doped layers. As explained in Sec. II, widths of the Be δ -doped potential wells at Fermi levels are only 1–2 nm in these samples according to the self-consistent calculations of electron states. These widths are considerably smaller than the magnetic length $(\hbar c/eB)^{1/2}$ associated with an applied field¹⁴ used in the present study. For example the magnetic length of 9 T is approximately 7 nm. Such small widths inhibit effective coupling of the parallel magnetic field to the orbital motion of carriers in the δ -doped layer and give rise to the possibility of the manifestation of the effect of spins in the parallel field magnetoresistance. In the case of a magnetic field perpendicular to the δ -doped layer, on the other hand, the coupling of the applied field to the orbital motion of carriers gives rise to monotonic positive magnetoresistance in these samples in which significant phonon and impurity scattering of carriers occur.

If a magnetic field is applied to a paramagnetic material with localized spins in the direction parallel to the current, negative magnetoresistance occurs as a result of the alignment of localized spins by the applied magnetic field which reduces spin-disorder scattering of carriers. The negative magnetoresistance due to this effect increases at lower temperatures where the effect of the applied magnetic field prevails over that of thermal disorder of spins. As stated in the Introduction, strongly localized holes in Be δ -doped layers are expected to form hydrogenic states at Be atoms and result in the existence of localized spins. Similar negative magnetoresistance is, therefore, expected to occur in our samples by a magnetic field parallel to the δ -doped layer. The spin-disorder scattering resistivity ρ_s is given by^{15,16}

$$\rho_s = 2\pi^2 \frac{k_F m^2 J^2}{pe^2 h^3} n_s [S(S+1) - \langle S \rangle^2], \quad (1)$$

where k_F is the Fermi wave number, m the effective mass of a carrier, J the exchange integral, p the carrier concentration, n_s the density of the localized spin, S the localized spin, and $\langle S \rangle$ the thermal average of the localized spin. At sufficiently high temperatures, where correlation between localized spins becomes negligible, the thermal average of localized spins $\langle S \rangle$ becomes proportional to B/T and, hence, negative magnetoresistance is proportional to B^2/T^2 according to Eq. (1). In insulating samples such as Be/LT-2, the carrier concentration changes significantly with the temperature due to thermal excitation of carriers. Their resistivity, hence, changes with the temperature due to this effect. The resistivity of the sample Be/LT-1, on the other hand, remains nearly constant over the wide temperature range as seen in Fig. 2, indicating that its carrier concentration is nearly constant. In Fig. 5(b) negative magnetoresistance of this sample is plotted as a function of $1/T^2$, which shows a nearly linear change in the high-temperature side. Our results shown in Fig. 4(b) and 4(c) and in Fig. 5(b), therefore, nearly satisfy the above-mentioned relation, which provides a further indication for localized spins as the origin of the negative magnetoresistance. By assuming that each hydrogenic state at a Be atom has a localized spin $S=\frac{1}{2}$, one may be able to estimate the magnitude of the exchange integral J in Eq. (1) from the data

shown in Fig. 5(b). We, however, do not know accurate values of k_F of this sample and the Landé g factor of this system. If we further assume that the Fermi wavelength λ_F is a few nm, corresponding to the Fermi energy of a few tens meV,⁹ and g is approximately 8 as in the case of localized spins in Zn doped GaAs,⁶ J is estimated as several tens eV Å³. This value is in the same order of magnitude of J estimated from negative magnetoresistance data of $\text{Ga}_x\text{Mn}_{1-x}\text{As}$.¹⁶

In an earlier study on hopping conduction in Si δ -doped layers in GaAs, negative magnetoresistance was observed with magnetic fields perpendicular to the δ -doped layers.¹⁷ The origin of the negative magnetoresistance in this earlier study whose magnetotransport measurements were carried out at 4.5 K was explained with a destructive interference of electron paths. In the present case negative magnetoresistance was observed at far higher temperatures and, hence, cannot be ascribed to the same origin.

The change of the parallel field magnetoresistance from negative to positive values at low temperatures may be ascribed in part to a gradual increase in the contribution of the hopping conduction which is known to give rise to large positive magnetoresistance. The bumps of curves of the temperature dependence of the parallel field magnetoresistance, however, suggest a possibility of the occurrence of another process at these temperatures; the positive magnetoresistance of hopping conduction monotonically increases by the lowering temperature¹³ and hence cannot give rise to these bumps. Such a process is likely to be associated with localized spins because bumps are observed only in curves of the

parallel field magnetoresistance. Antiferromagnetic coupling of localized spins associated with hydrogenic impurity states is known to occur at their high concentrations.⁷ There is, therefore, possibility that these bumps may result from antiferromagnetic alignments of localized spins in the δ -doped layers. Resistivity maxima which are seen in Fig. 3(a) are located at temperatures close to those where bumps occur in parallel field magnetoresistance. They may also be related to antiferromagnetic alignments of localized spins.

In summary, the present paper reports results of magnetotransport measurements of Be δ -doped GaAs structures in which holes exist only at deep levels of δ -doped layers. With the results presented here, it is reasonable to conclude that the negative magnetoresistance observed in the high temperature range under parallel magnetic fields results from localized spins associated with these holes. Up to the present, dopant impurities which have been known to give rise to localized spins in III-V and group IV semiconductors at high temperatures are only transition-metal and rare-earth elements. In the present results, the occurrence of antiferromagnetic alignments of localized spins at low temperatures is also suggested by the observation of bumps on the curves of the parallel field magnetoresistance, but a further experimental study is necessary in order to substantiate such possibility.

ACKNOWLEDGMENT

The authors thank Y. Yamamoto, H. Iwasaki, and H. Hori for valuable discussions.

*Corresponding author; FAX: 81-761-51-1149; Electronic address: otsuka@jaist.ac.jp

¹H. Munekata, H. Ohno, S. von Molnár, A. Segmüller, L. L. Chang, and L. Esaki, Phys. Rev. Lett. **63**, 1849 (1989).

²H. Ohno, A. Shen, F. Matsukura, A. Oiwa, A. Endo, S. Katsumoto, and Y. Iye, Appl. Phys. Lett. **69**, 363 (1996).

³H. Ohno, D. Chiba, F. Matsukura, T. Omiya, E. Abe, T. Dietl, Y. Ohno, and K. Ohtani, Nature (London) **408**, 944 (2000).

⁴G. Feher, Phys. Rev. **114**, 1219 (1959).

⁵G. Feher, J. C. Hensel, and E. A. Gere, Phys. Rev. Lett. **5**, 309 (1960).

⁶R. S. Title, IBM J. Res. Dev. **7**, 68 (1963).

⁷D. Jérôme and J. M. Winter, Phys. Rev. **134**, A1001 (1964).

⁸J. P. Noh, F. Shimogishi, and N. Otsuka, Phys. Rev. B **67**, 075309 (2003).

⁹J. P. Noh, F. Shimogishi, Y. Idutsu, and N. Otsuka, Phys. Rev. B **69**, 045321 (2004).

¹⁰Y. Idutsu, F. Shimogishi, J. P. Noh, and N. Otsuka, J. Vac. Sci. Technol. B **24**, 157 (2006).

¹¹M. Shinada and S. Sugano, J. Phys. Soc. Jpn. **21**, 1936 (1966).

¹²J. M. Ferreyra and C. R. Proetto, Phys. Rev. B **44**, 11231 (1991).

¹³B. I. Shklovskii and A. L. Efros, *Electronic Properties of Doped Semiconductors* (Springer, Berlin, 1984).

¹⁴S. Das Sarma and E. H. Hwang, Phys. Rev. Lett. **84**, 5596 (2000).

¹⁵P. G. de Gennes and J. Friedel, J. Phys. Chem. Solids **4**, 71 (1958).

¹⁶F. Matsukura, H. Ohno, A. Shen, and Y. Sugawara, Phys. Rev. B **57**, R2037 (1998).

¹⁷Q. Y. Ye, A. Zrenner, F. Koch, and K. Ploog, Semicond. Sci. Technol. **4**, 500 (1989).